Determination of the stiffness tensor of a fractured medium using finite-element simulations

Juan E. Santos ,† José M. Carcione * and Stefano Picotti*

† CONICET, Instituto del Gas y del Petróleo, Universidad de Buenos Aires, Argentina and Department of Mathematics, Purdue University.

* Istituto Nazionale di Oceanografia e di Geofisica Sperimentale - OGS,Trieste, Italy

82th SEG Annual Meeting, Las Vegas, Nevada, November 5, 2012

Fractured media. I

- **Fractures** are common in the earth's crust due to different factors, for instance, tectonic stresses and natural or artificial hydraulic fracturing caused by a pressurized fluid.
- **Seismic wave propagation** through **fractures and cracks** is an important subject in exploration and production geophysics, earthquake seismology and mining.
- **Fractures** constitute the sources of earthquakes, and hydrocarbon and geothermal reservoirs are mainly composed of **fractured rocks**.

Fractured media. II

- Modeling fractures requires a suitable interface model. Schoenberg (JASA (1980), GP (1983)) proposed the so-called linear-slip boundary condition model (LSBC), based on the discontinuity of the displacement and the continuity of the stress components across the fractures. (Schoenberg's model).
- A generalization of the (LSBC) (Carcione, JGR (1996)) states that across a fracture stress components are proportional to the displacement and velocity discontinuities through specific stiffnesses and viscosities, respectively.

Fractured media. III

- Displacement discontinuities conserve energy, while velocity discontinuities generate energy loss at the fractures. The specific viscosity accounts for the presence of a liquid under saturated conditions, introducing a viscous coupling between both sides of a fracture.
- Schoemberg's theory predicts that a dense set of parallel plane fractures behaves as a Transversely Isotropic Viscoelastic (TIV) medium if the dominant wavelength of the traveling waves is much larger than the distance between the fractures.

Fractured media. IV

- **Schoenberg's model** has never been simulated with a numerical method.
- To test the theory, in the context of **Numerical rock physics** we developped a **novel numerical solver** that can be used in more general situations.
- **Numerical rock physics** offer an alternative to laboratory measurements.
- **Numerical experiments** are **inexpensive, repeatable**, essentially free from experimental errors and can easily be run using alternative models of the materials being analized.

Fractured media. V

- To determine the complex stiffness coefficients of the equivalent TIV medium, we solve a set of boundary value problems (BVP's) for the wave equation of motion in the frequency-domain using the finite-element method (FEM).

- The BVP's represent harmonic tests at a finite number of frequencies on a sample having a dense set of fractures, modeled using the LSBC.

The equivalent TIV medium. I

Consider a viscoelastic isotropic background medium having a set of parallel (horizontal) fractures and its description in the space-frequency domain.

$\mathbf{u}$, $e_{ij}(\mathbf{u})$, $\sigma_{ij}(\mathbf{u})$: frequency domain displacement vector, strain components and stress components of the background medium.

The stress-strain relations and equations of motion:

$$\sigma_{jk}(\mathbf{u}) = \lambda \delta_{jk} \nabla \cdot \mathbf{u} + 2\mu e_{jk}(\mathbf{u})$$

$$\rho\omega^2 \mathbf{u}(x,z,\omega) + \nabla \cdot \sigma[\mathbf{u}(x,z,\omega)] = 0$$

δ_{jk}: Kroenecker delta λ, μ: complex Lamé constants ρ: mass density.

The equivalent TIV medium. II

x_1 and x_3: horizontal and vertical coordinates, respectively. When a **dense set of parallel fractures** is present, the medium behaves as a **TIV medium** at long wavelengths. τ_{ij}, ϵ_{ij}: stress and strain tensors of the equivalent TIV medium. **Stress-strain relations:**

$$\tau_{11}(\mathbf{u}) = p_{11}\,\epsilon_{11}(\mathbf{u}) + p_{12}\,\epsilon_{22}(\mathbf{u}) + p_{13}\,\epsilon_{33}(\mathbf{u}),$$
$$\tau_{22}(\mathbf{u}) = p_{12}\,\epsilon_{11}(\mathbf{u}) + p_{11}\,\epsilon_{22}(\mathbf{u}) + p_{13}\,\epsilon_{33}(\mathbf{u}),$$
$$\tau_{33}(\mathbf{u}) = p_{13}\,\epsilon_{11}(\mathbf{u}) + p_{13}\,\epsilon_{22}(\mathbf{u}) + p_{33}\,\epsilon_{33}(\mathbf{u}),$$
$$\tau_{23}(\mathbf{u}) = 2\,p_{55}\,\epsilon_{23}(\mathbf{u}),$$
$$\tau_{13}(\mathbf{u}) = 2\,p_{55}\,\epsilon_{13}(\mathbf{u}), \quad \tau_{12}(\mathbf{u}) = 2\,p_{66}\,\epsilon_{12}(\mathbf{u}).$$

The equivalent TIV medium. III

Schoenberg's theory predicts that if the background medium is homogeneous, the stiffnesses p_{IJ}'s are given by

$$p_{11} = p_{22} = E - \lambda^2 Z_N c_N, \quad p_{12} = \lambda - \lambda^2 Z_N c_N, \; p_{13} = \lambda c_N,$$

$$p_{33} = E c_N, \quad p_{55} = \mu c_T, \quad p_{66} = \mu.$$

where $E = \lambda + 2\mu$ **,**

$$c_N = (1 + E Z_N)^{-1} \quad c_T = (1 + \bar{Z}_T)^{-1}.$$

Z_N and Z_T: normal and tangential complex compliances of the fractures

The equivalent TIV medium. IV

- **The theory assumes a constant background, that the distance between fractures is much smaller than the wavelength of the signal and that the boundary condition is the same for all the fractures.**
- **The numerical solver may consider an inhomogeneous background medium and dissimilar boundary conditions at the fractures surfaces.**
- **The p_{IJ}'s are the complex and frequency-dependent stiffnesses to be determined numerically with the harmonic experiments.**

Determination of the stiffness components p_{IJ}

$\Omega = (0, D)^2$: **a square sample of boundary**
$\Gamma = \Gamma^L \cup \Gamma^R \cup \Gamma^B \cup \Gamma^T$

$\Gamma^{(f,n)}, n = 1, \cdots, J^{(f)}$: **a set of horizontal fractures in** Ω**, each one of length** D**.**

This set of fractures decomposes Ω **in a set of nonoverlapping rectangles** $R^{(n)}, n = 1, \cdots, J^f + 1$**:**

$$\Omega = \cup_{n=1}^{J^{(f)}+1} R^{(n)}.$$

Boundary conditions at the fractures. I

$R^{(n)}$ **and** $R^{(n+1)}$**: two rectangles having as a common side the fracture** $\Gamma^{(f,n)}$**.**

$\nu_{n,n+1}$**: the unit outer normal on** $\Gamma^{(f,n)}$ **from** $R^{(n)}$ **to** $R^{(n+1)}$

$\chi_{n,n+1}$**: a unit tangent on** $\Gamma^{(f,n)}$ **oriented counterclockwise.**

$\mathbf{u}^{(n)} = \mathbf{u}|_{R^{(n)}}$**: restriction of u to** $R^{(n)}$**,**

$$[\mathbf{u}] = \left(\mathbf{u}^{(n)} - \mathbf{u}^{(n+1)}\right)|_{\Gamma^{(f,n)}} : \quad \textbf{jump of} \quad \mathbf{u} \textbf{ at } \Gamma^{(f,n)}$$

Boundary conditions at a fracture $\Gamma^{(f,n)}$. II

1. -continuity of the stress components

2.- stress components are proportional to the displacement and velocity discontinuities through specific stiffnesses and viscosities, respectively:

$$\sigma(\mathbf{u}^{(n)})\boldsymbol{\nu}_{n,n+1} = \sigma(\mathbf{u}^{(n+1)})\boldsymbol{\nu}_{n,n+1}, \quad \Gamma^{(f,n)},$$

$$\sigma(\mathbf{u}^{(n)})\boldsymbol{\nu}_{n,n+1} \cdot \boldsymbol{\nu}_{n,n+1} = (LZ_N^n)^{-1}[\mathbf{u}] \cdot \boldsymbol{\nu}_{n,n+1}, \quad \Gamma^{(f,n)},$$

$$\sigma(\mathbf{u}^{(n)})\boldsymbol{\nu}_{n,n+1}, \cdot \boldsymbol{\chi}_{n,n+1} = (LZ_T^n)^{-1}[\mathbf{u}] \cdot \boldsymbol{\chi}_{n,n+1}, \quad \Gamma^{(f,n)}.$$

L**: average distance between the fractures.**

Boundary conditions at the fractures. III

The compliances Z (Z_N or Z_T) are complex and frequency-dependent and can be expressed as

$$Z^{-1} = L(\kappa + \mathrm{i}\omega\eta),$$

where

κ is a specific stiffness with dimension of stiffness per unit length

η is a specific viscosity, having dimension of viscosity per unit length.

Determination of the stiffness components p_{IJ}. I

p_{33}: solve the viscoelastic wave equation in Ω using the fracture B. C.'s with the additional B. C.'s

$$\sigma(\mathbf{u})\nu \cdot \nu = -\Delta P, \quad \Gamma^T,$$
$$\sigma(u)\nu \cdot \chi = 0, \quad \Gamma,$$
$$\mathbf{u} \cdot \nu = 0, \quad \Gamma^L \cup \Gamma^R \cup \Gamma^B.$$

In this experiment $\epsilon_{11}(\mathbf{u}) = \epsilon_{22}(\mathbf{u}) = 0$.

Determination of the stiffness components p_{IJ}. II

V: **original volume of the sample**

$\Delta V(\omega)$: **complex oscillatory volume change.**

In the quasistatic case

$$\frac{\Delta V(\omega)}{V} = -\frac{\Delta P}{p_{33}(\omega)}.$$

Using the average vertical displacement $u_3^{s,T}(\omega)$ **suffered by the boundary** Γ^T **and the the estimate**

$$\Delta V(\omega) \approx D u_3^{s,T}(\omega)$$

allows us to determine $p_{33}(\omega)$**.**

Determination of the stiffness components p_{IJ}. III

p_{11}: solve the viscoelastic wave equation with the fracture B. C.'s and the additional B. C.'s

$$\sigma(\mathbf{u}) \cdot \nu \cdot \nu = -\Delta P, \quad \Gamma^R,$$
$$\sigma(\mathbf{u}) \cdot \nu \cdot \chi = 0, \quad \Gamma,$$
$$\mathbf{u} \cdot \nu = 0, \quad \Gamma^L \cup \Gamma^B \cup \Gamma^T.$$

Here $\epsilon_{33} = \epsilon_{22} = 0$ and this experiment determines p_{11} computing the volume change as indicated for p_{33}.

Determination of the stiffness components p_{IJ}. IV

p_{55}: solve the viscoelastic wave equation with the fracture B. C.'s and the additional B. C.'s

$$\sigma \cdot \chi = \mathbf{g}, \quad \Gamma^T \cup \Gamma^L \cup \Gamma^R,$$
$$\mathbf{u} = 0, \quad \Gamma^B,$$

$$\mathbf{g} = \begin{cases} (0, \Delta G), & \Gamma^L, \\ (0, -\Delta G), & \Gamma^R, \\ (\Delta G, 0), & \Gamma^T. \end{cases}$$

$\theta(\omega)$: angle between the original positions of the lateral boundaries and their location after applying the shear stresses.

Determination of the stiffness components p_{IJ}. V

To estimate $\theta(\omega)$, compute the average horizontal displacement $\mathbf{u}_1^T(\omega)$ at the boundary Γ^T and use that

$$\tan[\theta(\omega)] \approx \mathbf{u}_1^T(\omega)/D.$$

Thus, the change in shape of the rock sample allow us to determine $p_{55}(\omega)$ from the relation (Kolsky, 1963)

$$\tan[\theta(\omega)] = \frac{\Delta G}{p_{55}(\omega)}.$$

p_{66}: Since this stiffness is associated with shear waves traveling in the (x_1, x_2)-plane, we rotate the layered sample 90 degrees and apply the shear test as indicated for p_{55}.

Determination of the stiffness components p_{IJ}. VI

p_{13}: solve the viscoelastic wave equation with the fracture B. C.'s and the additional B. C.'s

$$\sigma(\mathbf{u}) \cdot \nu \cdot \nu = -\Delta P, \quad \Gamma^R \cup \Gamma^T,$$
$$\sigma(\mathbf{u}) \cdot \nu \cdot \chi = 0, \quad \Gamma,$$
$$\mathbf{u} \cdot \mathbf{n} = 0, \quad \Gamma^L \cup \Gamma^B.$$

In this experiment $\epsilon_{22} = 0$, and from the stress-strain relations at the macroscale we get

Determination of the stiffness components p_{IJ}. VII

$$\tau_{11} = p_{11}\epsilon_{11} + p_{13}\epsilon_{33},$$

$$\tau_{33} = p_{13}\epsilon_{11} + p_{33}\epsilon_{33},$$

$\epsilon_{11}, \epsilon_{33}$: **macroscopic strain components at the right lateral side (Γ^L) and top side (Γ^T) of the sample, respectively.**

Then using that $\tau_{11} = \tau_{33} = -\Delta P$ we obtain

$$p_{13}(\omega) = \frac{p_{11}\epsilon_{11} - p_{33}\epsilon_{33}}{\epsilon_{11} - \epsilon_{33}}.$$

Schematic representation of the oscillatory compressibility and shear tests in Ω

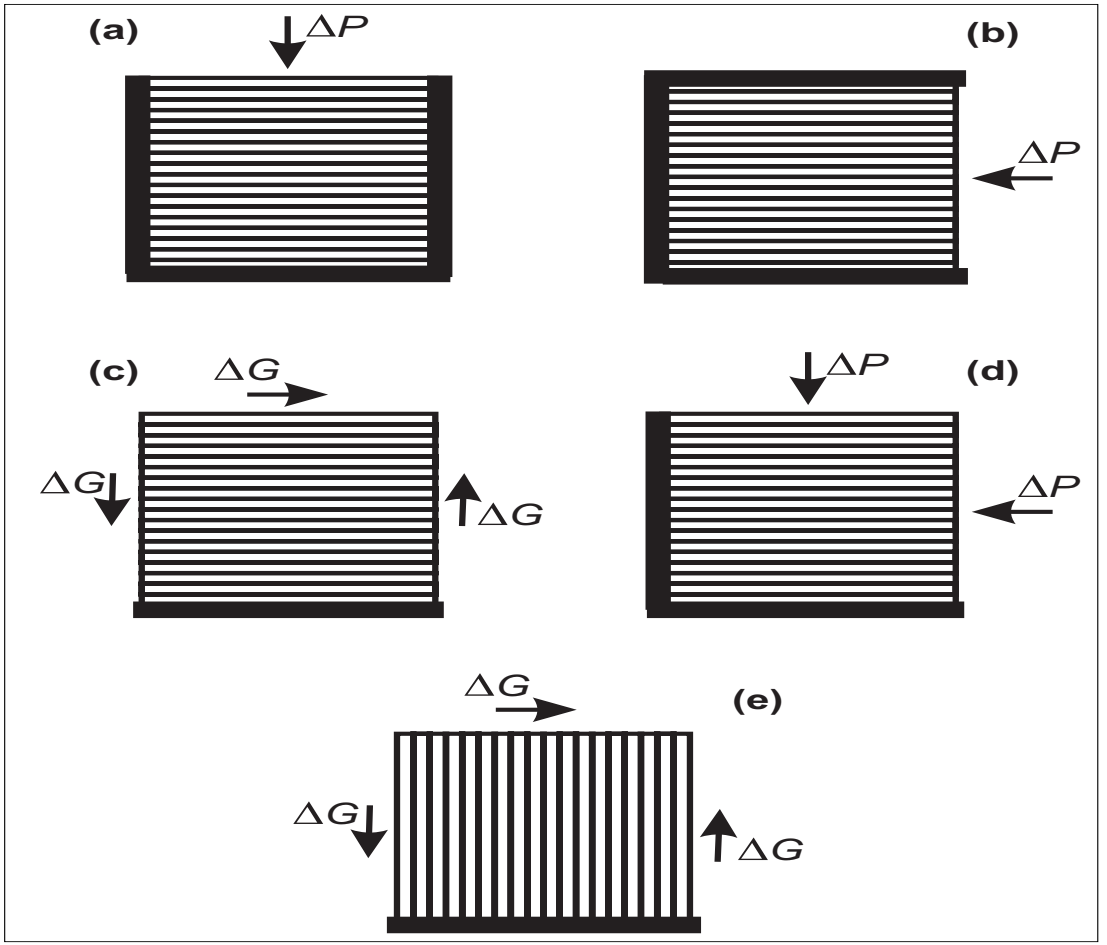

a): p_{33}, b): p_{11}, c): p_{55}, d): p_{13} e): p_{66}

Finite element implementation

The FE formulation uses bilinear elements to compute approximate solution of the bounday value problems, as explained in Santos et al. (CMAME, 2012), where apriori error estimates which are optimal for the regularity of the solution are given.

Numerical experiments. I

We consider the data provided by the laboratory experiments of Chichinina et al. (TPM, 2009), measured at 100 kHz.

Determination of reliable fracture parameters needs measurements at the seismic range.

The background medium is isotropic with

λ = 10 GPa, μ = 3.9 GPa and ρ = 2300 kg/m^3.

The simulations to determine the p_{IJ}'s used a square sample of side length 30 cm with 29 equally spaced fractures.

Numerical experiments. II

Fracture distance is L = 1 cm, grid spacing is h = 0.5 cm.

Experimental values of Z_N and Z_T for wet fractures scaled to seismic frequencies:

$$Z_N^{-1} = [34 + i(f/f_0)24.7]\,\mathbf{GPa}$$

$$Z_T^{-1} = [15.5 + i(f/f_0)11.3]\,\mathbf{GPa}$$

$$f_0 = 25\mathbf{Hz}.$$

Validation of the FE method. Phase velocities as function of frequency for wet fractures.

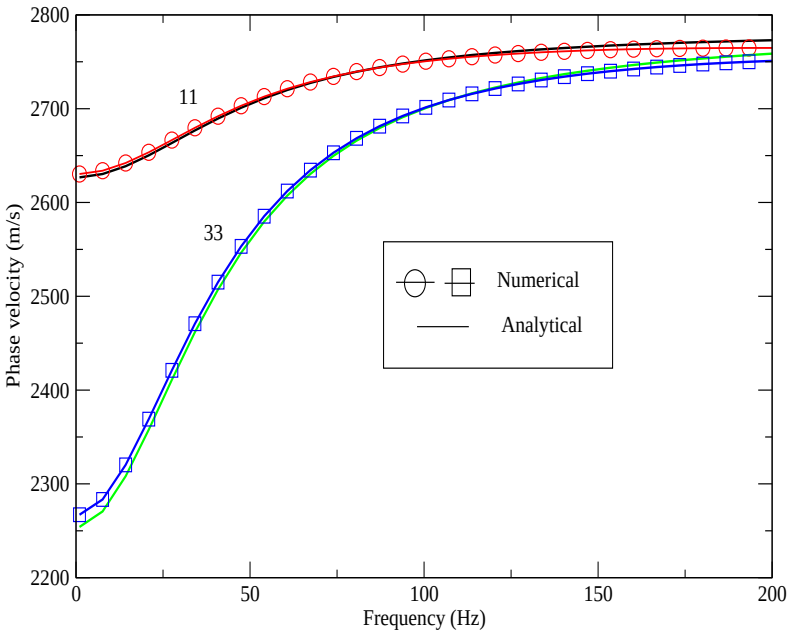

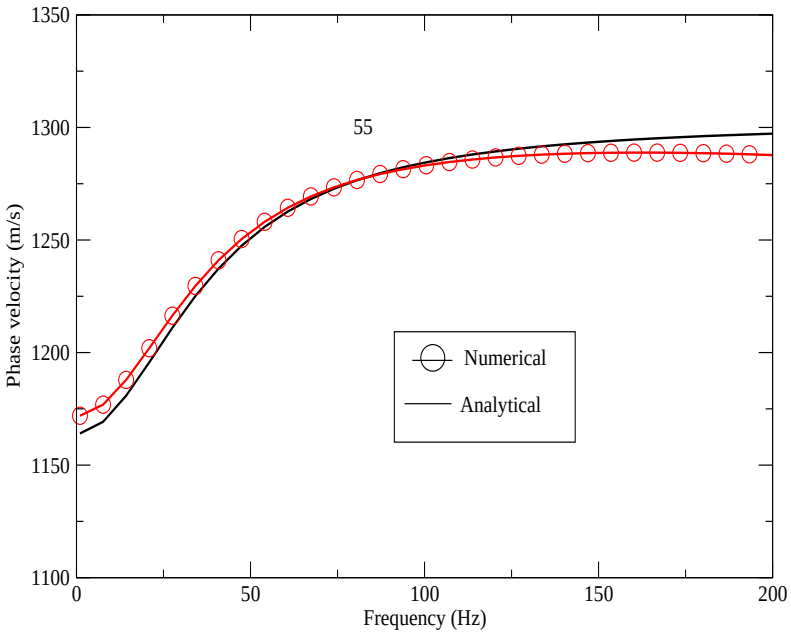

"11" and "33" refer to the qP wave along and perpendicular to the fracture plane. "55" refers to the qS wave perperdicular to the fracture plane. A very good fit is observed. qP waves along the fracture plane ("11") travel faster than qP waves travelling perpendicular to the fractures ("33").

Validation of the FE method. Dissipation factor as function of frequency for wet fractures.

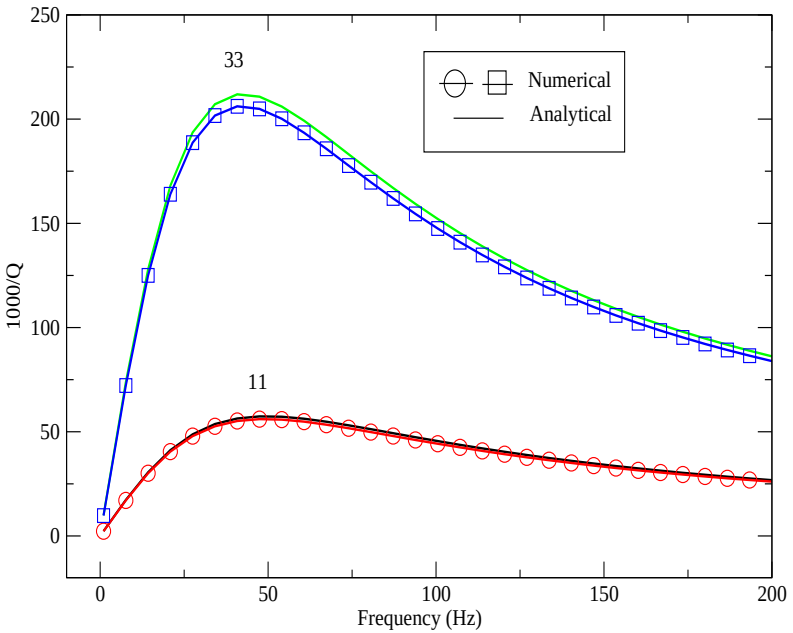

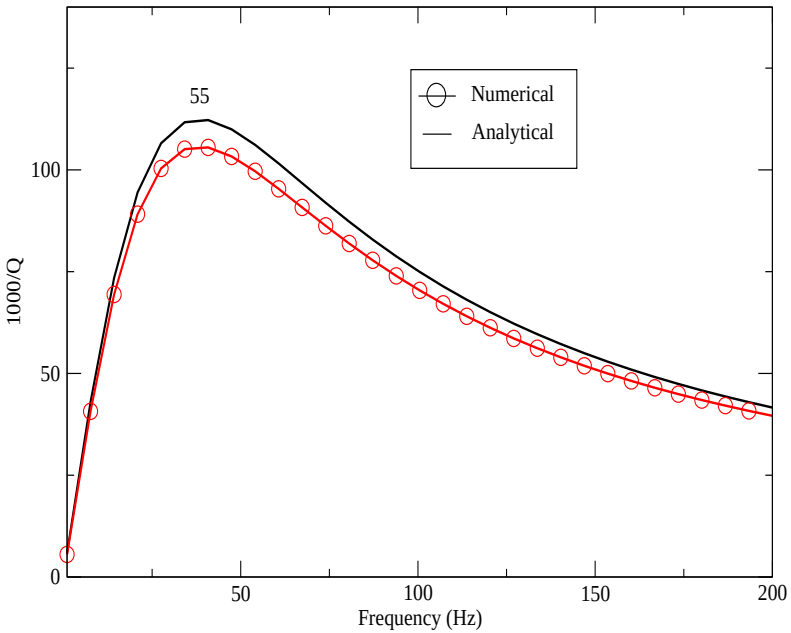

"11" and "33" refer to the qP wave along and perpendicular to the fracture plane. "55" refer to the qS wave perperdicular to the fracture plane. A very good fit is observed. qP waves along the fracture plane ("11") suffer lower attenuation than qP waves travelling perpendicular to the fractures ("33").

Fractures at varying pore fluid pressure .

Daley et a. (GPY, 2006) suggest to take high values of fracture compliance at low

effective normal stress $\sigma = pc - pp$**,**

where pc **is the confining pressure and** pp **the pore presure. For a contant** pc **= 30 MPa, we consider two pore pressures values: 5 MPa (normal) and 25 MPa (overpressure). Using their model, we obtain, at 25 Hz,**

$$pp = 5\text{MPa}, \;\; Z_N^{-1} = (23.1 + 5.9\text{i}), \; Z_T^{-1} = (75 + 9.4\text{i})(\text{GPa}),$$

$$pp = 28\text{MPa}, \;\; Z_N^{-1} = (14.4 + 3.6\text{i}), \; Z_T^{-1} = (21 + 2.6\text{i})(\text{GPa}).$$

We consider a set of equispaced fractures with L **= 1 cm and 80 % binary fractal variations of** Z_N **and** Z_T **around these mean values.**

Real part of fractal Z_N^{-1} at pore pressure 28 MPa.

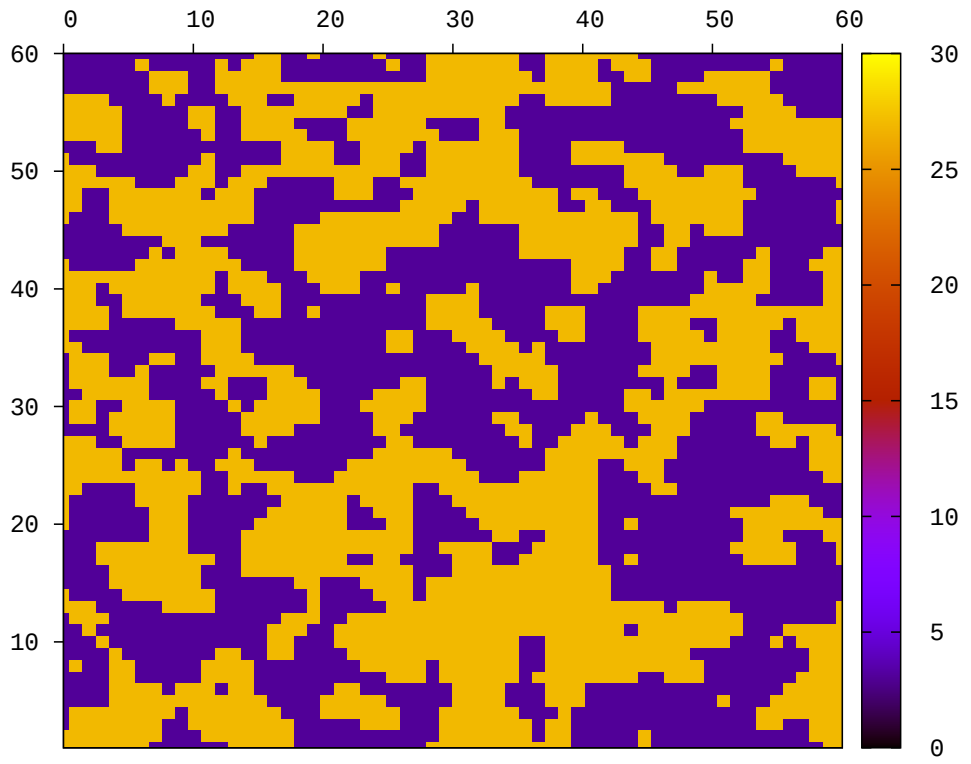

80 % binary fractal variations of Z_N around the mean value 23.1 GPa

Phase velocities for fractal ZN ZT, wet fractures. *pc* is 30 MPa. Pore pressures *pp*: 5 MPa and 28 MPa.

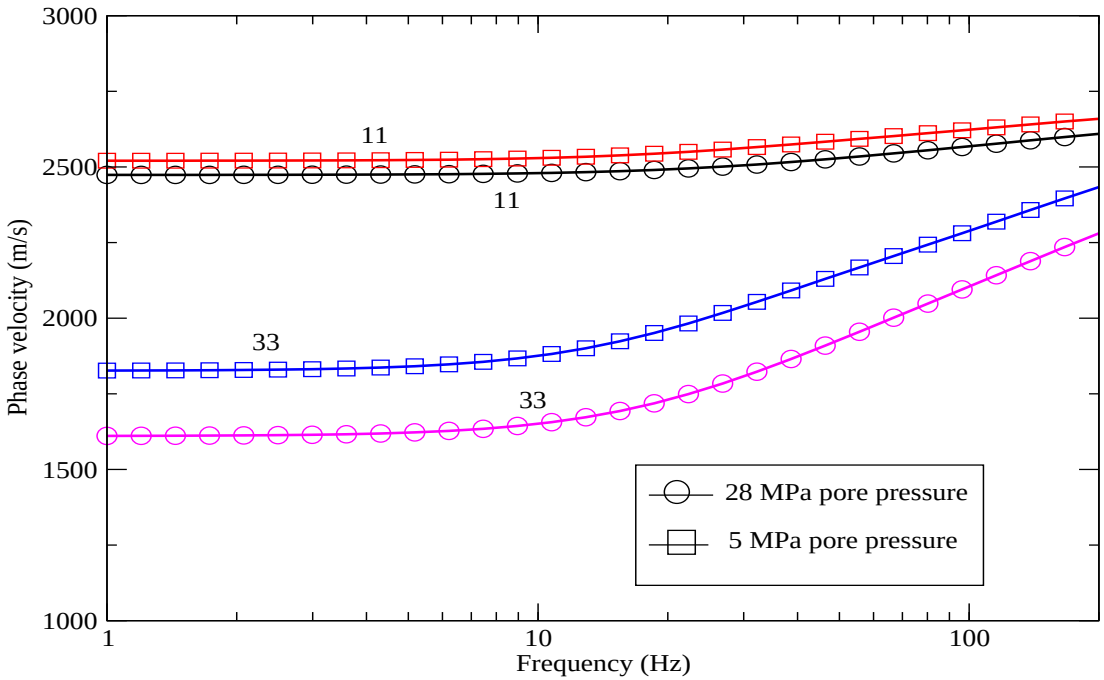

"11" and "33" refer to the qP wave along and perpendicular to the fracture plane. Higher pore pressure (circles) implies lower phase velocity. The "33" qP wave is the one more affected by overpressure.

Dissipation factor for fractal ZN ZT, wet fractures. *pc* is 30 MPa. Pore pressures *pp*: 5 MPa and 28 MPa.

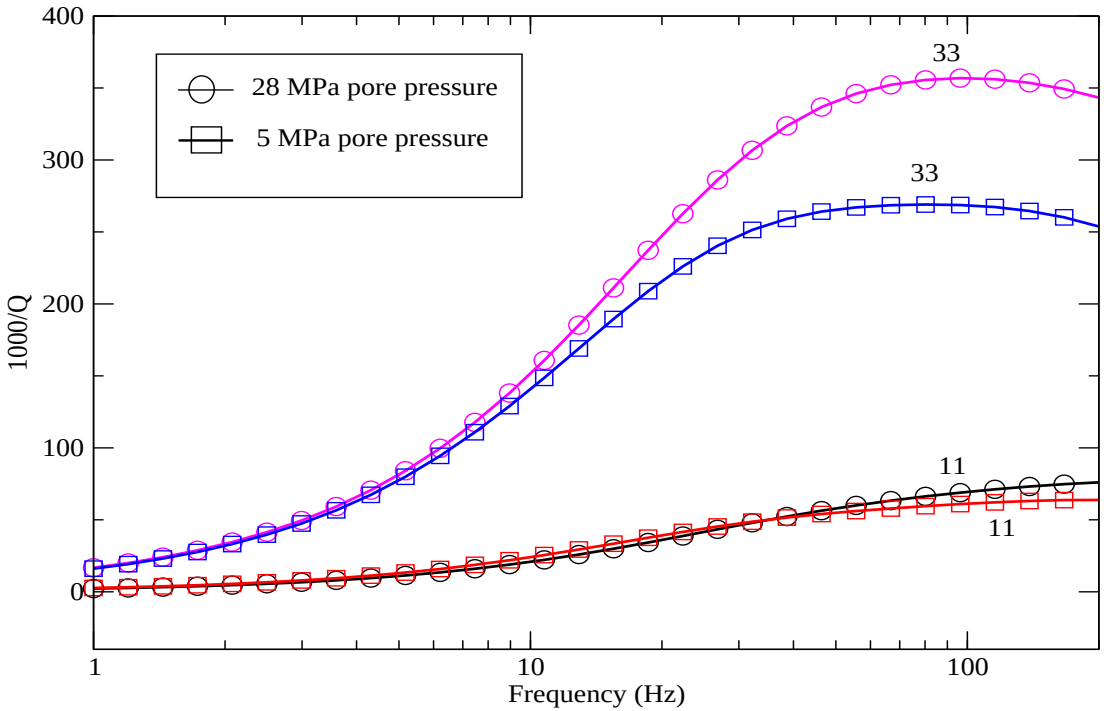

"11" and "33" refer to the qP wave along and perpendicular to the fracture plane.

Attenuation is stronger in the overpressured case (circles) for "33" waves.

Phase velocity for fractal and uniform ZN ZT, wet fractures. pc is 30 MPa. Pore pressure pp is 28 MPa (overpressure).

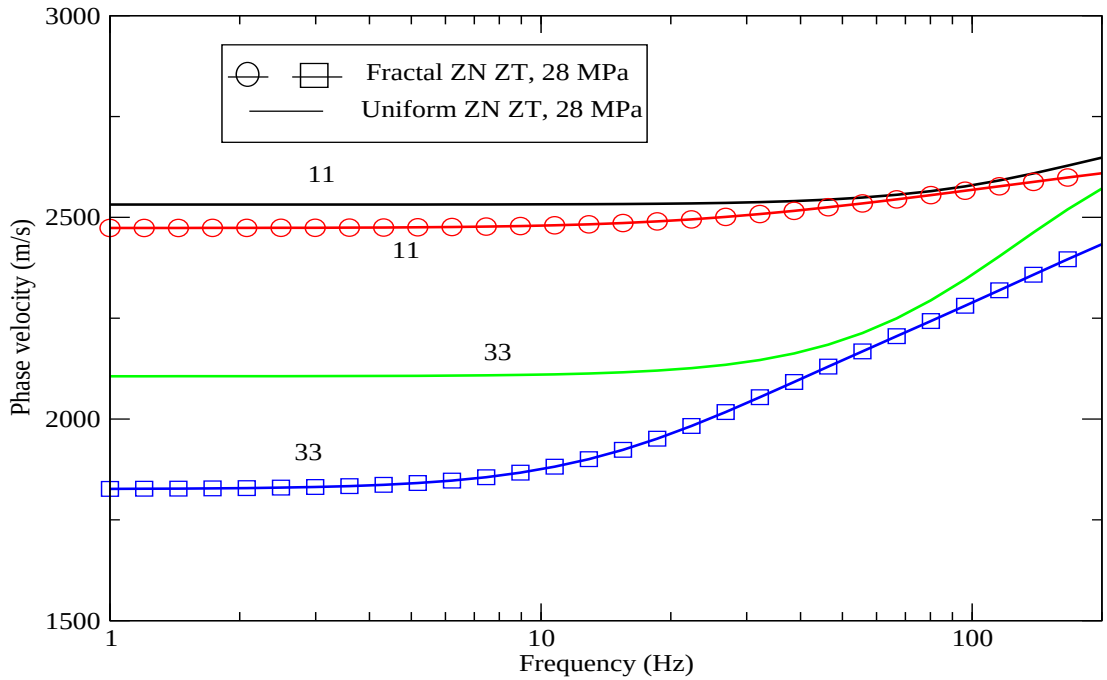

"11" and "33" refer to the qP wave along and perpendicular to the fracture plane. Phase velocities in the fractal case are lower than those obtained with the mean values. The "33" qP wave is the one more affected by the heterogeneities.

Dissipation factor for fractal and uniform ZN ZT, wet fractures. pc is 30 MPa. Pore pressure pp is 28 MPa (overpressure).

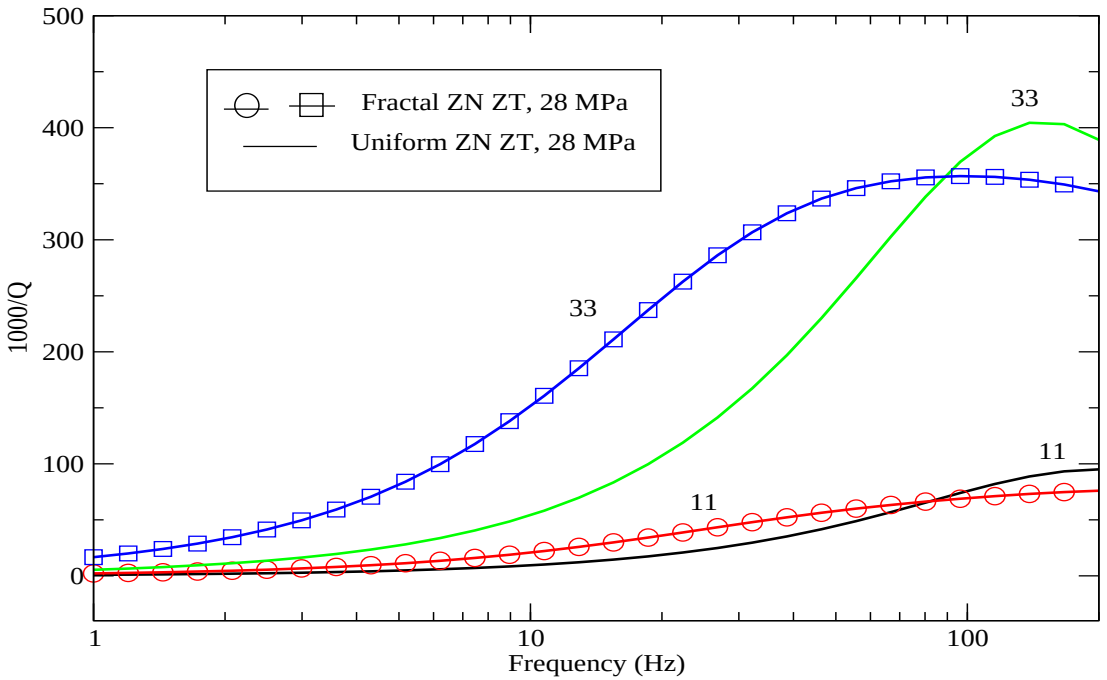

"11" and "33" refer to the qP wave along and perpendicular to the fracture plane. Dissipation factor of the "33" qP wave is more affected by the heterogeneities, showing lower values in the fractal case.

Fractal λ and μ background.

50 % binary fractal variations of the background Lamé constants λ and μ with respect to the mean values 10 GPa and 3.9 GPa, respectively.

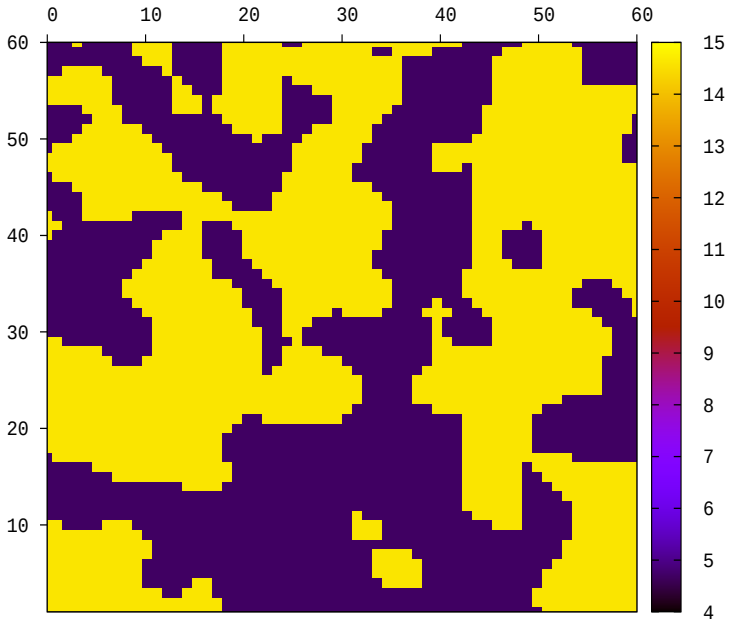

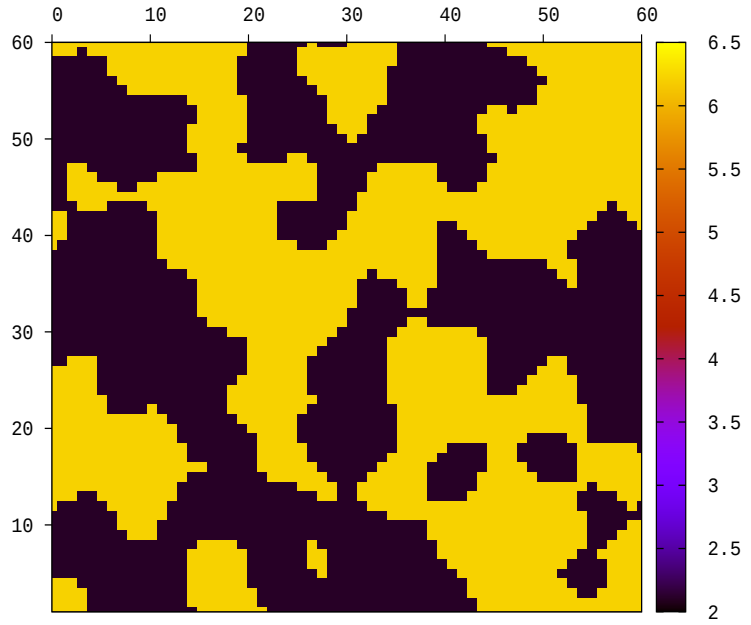

Phase velocities and dissipation. Uniform and fractal brackground, dry fractures.

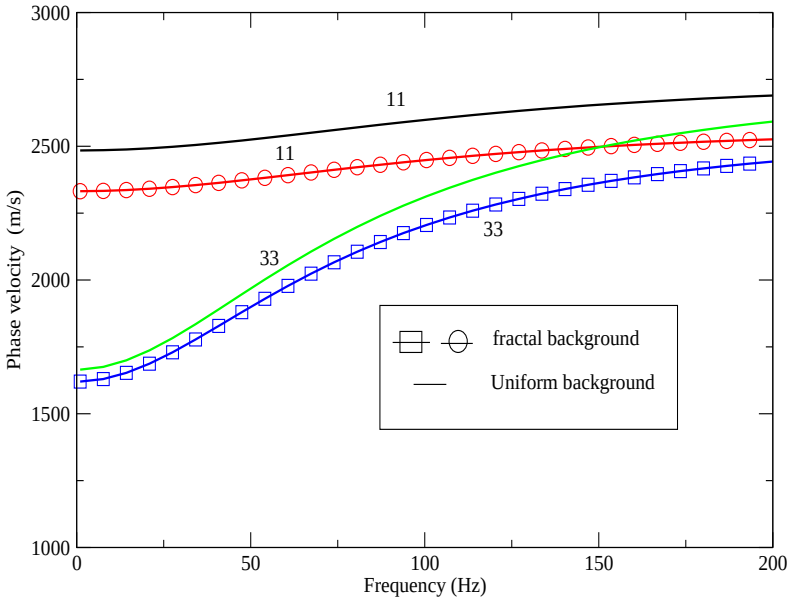

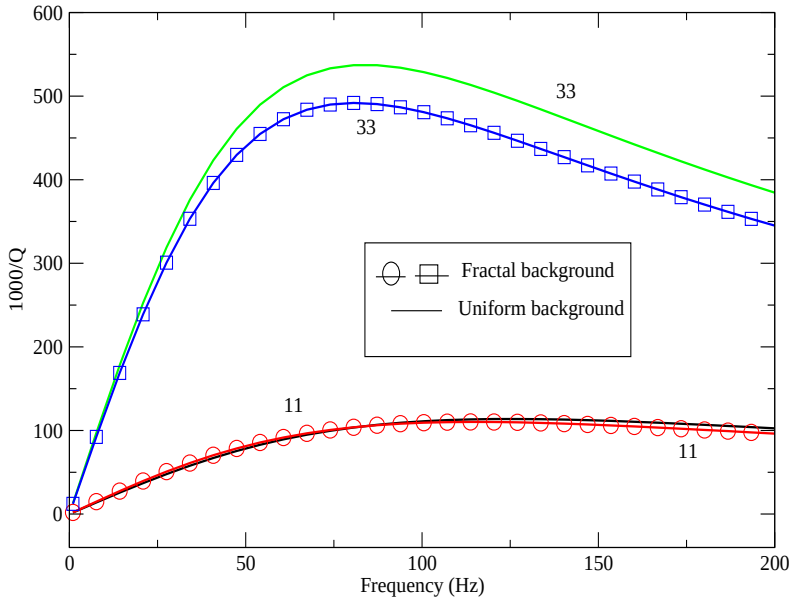

"11" and "33" refer to the qP wave along and perpendicular to the fracture plane. Phase velocities are lower for the fractal case for both "11" and "3 3" qP waves. Concerning attenuation, for qP "33" waves is lower than in the uniform background case, while attenuation for qP "11" waves is not affected by the fractal background. Fracture compliances: Z_N^{-1} **= 9.6 +** $\mathrm{i}(f/f_0)$ **4.8 GPa,** Z_T^{-1} **= 3.1+** $\mathrm{i}(f/f_0)$ **0.12 GPa.**

CONCLUSIONS. I

- Schoenberg's theory predicts that an homogeneous background containing a dense set of horizontal parallel fractures behaves like a TIV medium at long wavelengths.
- We presented a collection of novel FE harmonic experiments to test and validate the theory.
- The methodology was applied to cases when no analytical solutions are avalaible, such as fractal variations of the fracture compliances at different pore pressures and fractal Lamé parameters.

CONCLUSIONS. II

- In particular, it is shown that attenuation can be an indicator of overpressure with higher values at high pore pressures.
- THANKS FOR YOUR ATTENTION !!!!